

This is an open-access article distributed under the terms of the Creative Commons Attribution License, which permits unrestricted use, distribution, and reproduction in any medium, provided the original author(s) and source are credited.



ISSN: 0974-8369

Biology and Medicine

International, Open Access

Available online at: www.biolmedonline.com

This article was originally published in this journal and the attached copy is provided for the author's benefit and for the benefit of the author's institution, for commercial/research/educational use including without limitation use in instruction at your institution, sending it to specific colleagues that you know, and providing a copy to your institution's administrator.

All other uses, reproduction and distribution, including without limitation commercial reprints, selling or licensing copies or access, or posting on open internet sites, your personal or institution's website or repository, are requested to cite properly.

Electrodynamic Model of the Heart to Detect Necrotic Areas in a Human Heart

Veniamin Yur'evich Kazakov^{1,*}, Diana Konstantinovna Avdeeva¹, Michael Georgievich Grigoriev¹, Nataliya Mihajlovna Natalinova¹, Ivan Vadimovich Maksimov², Marija Vjacheslavovna Balahonova²

¹National Research Tomsk Polytechnic University, 30, Lenin Ave., Tomsk 634050, Russia

²RI Cardiology, 30, Kiyevskaya St., Tomsk 634012, Russia

Abstract

To diagnose the conditions and diseases of the cardiovascular system is the main task of electrocardiology. The problem of the cardiovascular system diagnostics is caused by a complex multi-level mechanism of its functioning, and only experienced specialists are able to establish a correct diagnosis. Since the working heart is inaccessible to direct observations in real life, diagnostics of diseases is based on noninvasive methods such as electrocardiography. By assumption, weak "bursts" (micropotentials) of electrocardiographic signals in different areas are the precursors of dangerous arrhythmias. The amplitude of these signals on the body surface is insignificant and tends to be commensurate with the noise level of the measuring system. Advances in electrocardiography make it possible to generate a high resolution ECG signal and to detect the heart micropotentials. The method of modeling helps to understand causes of micropotentials in the ECG signal by selecting the model parameters. The model of the heart should allow generating a signal close to the high resolution ECG signal. The research aims to find a numerical model that allows solving the inverse problem of the heart tissue characteristics recovery using a high resolution ECG signal and CT data on the heart geometry. The proposed computer model and highly sensitive methods for the ECG measurement are the part of the hardware-software complex to detect dangerous precursors of cardiac arrhythmias.

Keywords

Bioelectricpotentials of the heart; Biophysics of the heart cells; Cardiac conduction system; Electrodynamic activity of the heart; Micropotentials of the heart; Bidomain model of the heart; Localization of necrotic areas

Introduction

The heart is a complicated organ from both anatomical and physiological points of view. The fibrous skeleton, valve apparatus, endocardium, myocardium, conduction system, coronary and venous vessels, pericardium and nerve plexus relate to the anatomical structures of the heart. The heart is a hollow muscular organ separated by partitions into the left and right atria and right and left ventricles.

The atrial and ventricular myocardium consists of several layers of muscle fibers covering the internal cavities. The myocardium is composed of muscle cells of two types: contractile myocardium (cardiomyocytes) and specialized cells of the conduction system. Cardiomyocytes are connected to each other by intercalated disks and form myofibrils. Excitation easily passes from one cardiomyocyte to another through the disks (intercalated discs are electrical or chemical synapse). Muscle layers of the atria and ventricles are not directly connected to each other. The conduction system of the heart (Figure 1) is composed of sinus node, atrioventricular node and His-Purkinje system. The conduction system comprises cells of various types: P-type cells with a slow spontaneous depolarization, T-type cells (conducting cells) and others.

The main physiological functions of the heart can be summarized as follows: automatism, conduction, excitability, refractory, contractility. These functions are based on biochemistry and biophysics of the heart cells.

The description presented makes it possible to conclude that the heart is a complex dynamic system consisting of a large number of interacting subsystems of a complex geometric shape varying with time. In addition, there are individual features and age peculiarities of the heart and shape of the body.

The comprehensive study of the heart conducted in the second half of the XX century has led to the development of a separate scientific section known as biophysics of the heart to study the physical aspects of the heart activity at all levels, from molecules and cells to the whole cardiovascular system. One of the important practical applications of biophysical approaches in considering the heart function is the study of cardiac arrhythmia [2], which can cause sudden death. One of the significant methods to study arrhythmias and the underlying mechanisms is a method of computer simulation.

The reviews of computer modeling of the heart and cardiac activity can be found, for example, in [3,4].

The working heart is inaccessible to direct observation, so the diagnostics of diseases is based on noninvasive methods, electrocardiography being the most important one. By assumption, weak "bursts" (micropotentials) of electrocardiographic signals in different areas are the precursors of dangerous arrhythmias. The amplitude of these signals on the body surface is insignificant and tends to be commensurate with the noise level of the measuring system. Advances in electrocardiography make it possible to generate a high resolution ECG signal [5] and to detect the heart micropotentials. The method of modeling helps to understand causes of micropotentials in the ECG signal by selecting the model parameters. The model of the heart should allow generating a signal close to the high resolution ECG signal.

***Corresponding author:** Kazakov VY, National Research Tomsk Polytechnic University, 30, Lenin Ave., Tomsk 634050, Russia

Received: Dec 1, 2015; **Accepted:** Dec 21, 2015; **Published:** Jan 23, 2016

Citation: Kazakov VY, Avdeeva DK, Grigoriev MG, Natalinova NM, Maksimov IV, *et al.* (2015) Electrodynamic Model of the Heart to Detect Necrotic Areas in a Human Heart. Biol Med (Aligarh) 7(5): BM-155-15, 7 pages.

Copyright: © 2015 Kazakov *et al.* This is an open-access article distributed under the terms of the Creative Commons Attribution License, which permits unrestricted use, distribution, and reproduction in any medium, provided the original author and source are credited.

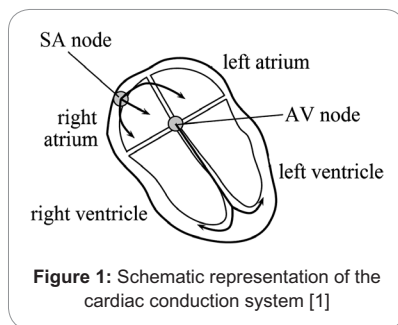


Figure 1: Schematic representation of the cardiac conduction system [1]

The research aims to find a numerical model that allows solving the inverse problem of the heart tissue characteristics recovery using a high resolution ECG signal with micropotentials of the heart and CT data on the heart geometry.

Methods

A standard mathematical model presented in [1] is used. A human body consists of billions of cells connected by various mechanisms of interaction depending on the type of tissue under consideration. The possible approach in constructing mathematical models for electrical activity in tissue is to model each cell separately and set the mechanism of their interaction. This approach is applicable only to very small samples of tissue due to the large number of cells. The present level of detailing is unachievable for the study of electrical phenomena at the level of organs or even organisms. Therefore, a standard approach of continuum mechanics to study the values averaged over a small volume is used. Such averaging can be used at the level of cells to obtain a continuous description of biological tissue. The selected scale of averaging is to be small in comparison with the typical size of the organ, but large if compared to the volume of a single cell. The values at each point of tissue are defined as average over the small but multicellular volumes in the point vicinity. Thus, we avoid difficulties in modeling the discrete structures of body tissue and can use a well-developed mathematical apparatus for differential calculus.

The simulation area can be divided into three parts (Figure 2): the heart, the body and the external environment. In this case, the determination of the electric potential distribution in the body and on the skin can be considered for T region with boundary conditions on ∂H and ∂T .

The electrical activity of the heart has frequencies in the range of up to 100 Hz, and the maximum frequencies are about 1 kHz, so the influence of finite speed of field propagation from the sources to

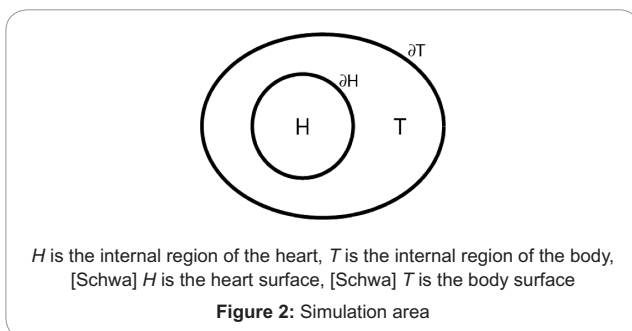


Figure 2: Simulation area

the points of observation and the influence of bias currents can be ignored [3]. This approximation is called quasi-static.

In the approximation of Maxwell's equations for the point with coordinates (x, y, z) , the equation for the potential can be represented as

$$\Delta u + \frac{1}{\sigma} \nabla \sigma \cdot \nabla u = \frac{1}{\sigma} \nabla \cdot (\sigma E_e) \quad (1)$$

where u is electrical scalar potential,

$[\text{Sigma}]$ is medium conductivity,

E_e is a field vector defined by nonelectric factors (chemical, thermal, etc.)

Let $J = [\text{Sigma}]E_e$ denote extraneous current vector. Vector J can be regarded as volume density of the dipole moment of the continuously distributed sources in the region with bioelectric generators.

Assuming that the human body has no bioelectric generators except for the heart, the equation and boundary conditions for the electric field potential in T region will take the form:

$$\Delta u_T + \frac{1}{\sigma} \nabla \sigma \cdot \nabla u_T = 0, \quad \vec{x} \in T \quad (2)$$

$$\vec{n} \cdot \sigma \frac{\partial u_T}{\partial \vec{n}} = 0 \quad (3)$$

$$u_T = u_{\partial H} \quad (4)$$

where u_T is the electric field potential inside the body,

\vec{n} is the vector of external normal to the body surface.

$U_{[\text{Schwa}]H}$ is the potential on the external surface of the heart. $U_{[\text{Schwa}]H}$ can be determined from the numerical solution of the model of the heart electrical activity inside the heart. The geometric shape of human body surface and the surface shape of the heart and the conductivity distribution inside the body are essential to close the system (2)-(4). The solution of the system will allow calculating the electric potential distribution inside the body $u_T(\vec{x})$ and on the external surface of a human torso, which is directly connected with electrocardiogram (ECG). If we know the potential distribution on the heart surface $u_{\partial H}(\vec{x})$ for different time points, we can calculate ECG signal on the body surface.

Modeling the electrical activity of the heart is based on the assumption that the heart tissue consists of two separate continuous regions: intracellular and extracellular. These regions are separated by the cell membrane. The laws of current conservation in quasi-static approximation of the electric field are used for the mathematical description of the tissue. This tissue model is called two-layer or bidomain [4]. Both domains are assumed to be continuous, filling the entire volume of the heart muscle. The muscle cells connected to each other by means of the so-called gap junctions allow considering the intracellular space as a continuous medium. Gap junctions are small channels embedded in the cell membrane to form a direct contact between the interior of two adjacent cells. Therefore, the substances like ions or small molecules may pass directly from one cell to another without passing through the space between the cells (extracellular domain). In these two regions we define the electric potential which should be considered as an averaged value over a small volume for each point.

The intracellular and extracellular domains are separated by the cell membrane. It is assumed that both domains are continuous and fill the entire volume of the heart. This assumption is applied to the cell membrane, which is also regarded as a continuous medium to fill the entire volume of the tissues. The membrane acts as an electrical insulator between the domains; otherwise, there will not be any potential difference between the domains. The membrane resistivity is high, but there are built-in channels with the electrically charged molecules (ions) capable of passing through the channels. Therefore, the electric current passes through the membrane and its value depends on the potential difference on the membrane and the membrane permeability for ions. The potential difference on the membrane is called transmembrane action potential (TAP). TAP is determined for each point of the heart.

Quasi-static approximation of Maxwell's equations is also correct for the heart tissue. The currents in the two domains can be represented as

$$J_i = -\sigma_i \nabla u_i \quad (5)$$

$$J_e = -\sigma_e \nabla u_e \quad (6)$$

where J_i and J_e are intracellular and extracellular currents, respectively,

σ_p, σ_e are domain conductivities,

u_p, u_e are the corresponding potentials.

Charge balance criterion for both sides of the membrane has the form:

$$\frac{\partial}{\partial t}(q_i + q_e) = 0 \quad (7)$$

Where q_i and q_e are intracellular and extracellular charges, respectively. The resulting current at each point of the heart tissue should be equal to the sum of the rate of charge accumulation on the opposite sides of the intercellular membrane of the point and ionic current through the membrane:

$$-\nabla \cdot J_i = \frac{\partial q_i}{\partial t} + \alpha \cdot I_{\text{ion}} \quad (8)$$

$$-\nabla \cdot J_e = \frac{\partial q_e}{\partial t} - \alpha \cdot I_{\text{ion}} \quad (9)$$

where I_{ion} is specific density of the ionic current through the membrane,

[alpha] characterizes the membrane surface area per unit volume.

Therefore, [alpha] I_{ion} is ionic current through the membrane per unit volume of the heart tissue. The positive direction of ionic current is considered to be the direction from the intracellular into extracellular space. On the basis of (5)-(9), we obtain

$$\nabla \cdot (\sigma_i \nabla u_i) + \nabla \cdot (\sigma_e \nabla u_e) = 0 \quad (10)$$

Introducing the transmembrane potential difference equal to $\nu = u_i - u_e$, we obtain the equation for the point of the heart tissue (standard formulation of the bimodal model) [6]:

$$\nabla \cdot (\sigma_i \nabla \nu) + \nabla \cdot (\sigma_e \nabla u_e) = \alpha C_m \frac{\partial \nu}{\partial t} + \alpha \cdot I_{\text{ion}} \quad (11)$$

$$\nabla \cdot (\sigma_i \nabla \nu) + \nabla \cdot ((\sigma_i + \sigma_{ie}) \nabla u_e) = 0 \quad (12)$$

where C_m is local membrane capacitance.

The conductive properties of the cardiac muscle tissue are anisotropic, so conductivities σ_p, σ_e are tensor quantities. The anisotropy is caused by the fact that the heart muscle is composed of fibers and conductivity in the longitudinal direction and is greater than in the transverse direction. In addition, the muscle fibers form layers and provide three distinct directions in the tissue conductance: parallel to fibers, perpendicular to fibers and parallel to the layer, and perpendicular to fibers and perpendicular to the layer. The fiber directions and therefore the conductivity tensor varies throughout the heart muscle. Three orthogonal unit vectors a_p, a_t and a_n are related to each point of the tissue, where vector a_i is located along fibers, a_t is perpendicular to fibers and lies in the layer plane, a_n is located perpendicular to fibers and normal to the muscular layer plane. The conductivity tensor M^* at a given point in the coordinate system a_p, a_t, a_n has a diagonal form:

$$M^* = \begin{bmatrix} \sigma_l & 0 & 0 \\ 0 & \sigma_t & 0 \\ 0 & 0 & \sigma_n \end{bmatrix} \quad (13)$$

In the global coordinate system, the conductivity tensor components have the form:

$$M_{ij} = a_i^j a_i^j \sigma_l + a_t^i a_t^i \sigma_t + a_n^i a_n^i \sigma_n \quad (14)$$

where $a_i^j, a_t^j, a_n^j, a_i^i, a_t^i, a_n^i (i, j = 1, 2, 3)$ are the components of decomposition of vectors a_p, a_t, a_n in the global coordinate system.

The parameters of the heart tissue are presented in Table 1.

Thus, if the ionic current distribution and distribution of the muscle fiber directions are given, we have all the necessary parameters. To close the system of equations (11)-(12), it is necessary to specify boundary conditions on the heart surface ∂H in the form:

$$n \cdot (\sigma_i \nabla \nu + \sigma_e \nabla u_e) = 0 \quad (15)$$

$$n \cdot (\sigma_e \nabla u_e) = n \cdot (\sigma_T \nabla u_T) \quad (16)$$

$$u_e = u_T \quad (17)$$

To simulate the process of activation and deactivation of the heart tissue, it is necessary to use realistic models of the ionic current. The existing models can be divided into three categories.

First, there are simple phenomenological models to reproduce the results of macroscopic observations of the cell behavior, for example, representation of the ionic current in the form of a cubic polynomial depending on the size of transmembrane potential.

C_m	1.0 $\mu\text{F}/\text{cm}^2$
α	2,000 cm^{-1}
σ_l^i	3.0 mS/cm
σ_t^i	1.0 mS/cm
σ_n^i	0.31525 mS/cm
σ_l^e	2.0 mS/cm
σ_t^e	1.65 mS/cm
σ_n^e	1.3514 mS/cm

Table 1: Parameters of the heart tissue

Secondly, there is a group of models often referred to as first-generation models. The group is an attempt to describe the observed cell behavior and its biophysics. These models consider the ionic currents which are important for action potential and use simplified formulations of the fundamental biophysical processes.

The third group of models is called second-generation models. The group provides very detailed description of the cell biophysics. The models are based on the advanced experimental methods to monitor small-scale parts of the cell physiology.

The purely phenomenological models can be useful to understand the qualitative behavior of the heart tissue. The full scope of modeling capabilities can be achieved only by using more complex models, since the purpose of mathematical and computer modeling is to study the mechanisms of the influence of physiology at the cellular level on the functions of the muscle tissue and the heart.

A large collection of the available cell models can be found on the CellML website [7]. Here, the extensible markup language XML is used to describe the models. In the database CellML, the cell models are regularly updated with regard to the latest achievements of the cell electrophysiology, contractile mechanisms and other physiological phenomena. The experimental methods are the basis for the cell models and they are constantly being developed resulting in further complication and more accurate description of the cell biophysics. The increased amount of the available data makes it possible to develop models that accurately describe the smallest details in the heart cell physiology.

In a normally functioning cell, several ionic currents cause changes in the transmembrane potential. The most important currents are transmembrane currents of sodium, potassium and calcium ions. The model for the total ionic current through the membrane can be developed on the basis of the description of each current using the equation (11):

$$I = G_{\max} O(\nu - \nu_{\text{eq}}), \quad (18)$$

where I is ionic current,

ν and ν_{eq} are transmembrane potential and equilibrium transmembrane potential for a given ion,

G_{\max} is maximum membrane conductivity if all the ionic channels are open,

O is the probability of a channel being open.

Classic model of ventricular cells is the Luo-Rudy model [8]. The Luo-Rudy model describes both the transmembrane potential and the dynamics of intracellular calcium concentration. The model consists of nine ordinary differential equations:

$$-C_m \frac{d\nu}{dt} = I_{\text{Na}} + I_{\text{si}} + I_{\text{K}} + I_{\text{K1}} + I_{\text{Kp}} + I_{\text{b}} + I_{\text{app}}; \quad (19)$$

$$\frac{dc_{\text{Ca}}}{dt} = -0.0001I_{\text{si}} + 0.07(0.0001 - C_{\text{Ca}}); \quad (20)$$

$$\frac{dg}{dt} = \alpha_g(1-g) - \beta_g g, \quad (21)$$

where $g = m, h, j, f, X, X_i$ are the variables to control ionic currents,

I_{Na} is fast sodium current,

I_{si} is slow calcium current inside the cell,

I_{K} is potassium current outside the cell, time-invariant,

I_{K1} is potassium current outside the cell, time-dependent,

I_{Kp} is potassium current outside the cell on the plateau of the transmembrane action potential,

I_{b} is background current similar to the leak current in the Hodgkin-Huxley model.

The complete specification of the model parameters including the equations for ionic currents is presented in [8].

Consider the final mathematical model for the electrical activity of the heart and the surrounding body of the patient. The ionic current through the cell membrane is of great importance for the cell activation in the heart tissue, so the model comprises a mathematical description of the cell membrane physiology. The full model is as follows:

$$\frac{\partial s}{\partial t} = F(s, \nu, t), \quad \bar{x} \in H; \quad (22)$$

$$\nabla \cdot (\sigma_i^* \nabla \nu) + \nabla \cdot (\sigma_e^* \nabla u_e) = \frac{\partial \nu}{\partial t} + I_{\text{ion}}^*, \quad \bar{x} \in H; \quad (23)$$

$$\nabla \cdot (\sigma_i^* \nabla \nu) + \nabla \cdot ((\sigma_i^* + \sigma_e^*) \nabla u_e) = 0, \quad \bar{x} \in H; \quad (24)$$

$$\nabla \cdot (\sigma_T^* \nabla u_T) = 0, \quad \bar{x} \in T; \quad (25)$$

$$u_e = u_T, \quad \bar{x} \in \partial H; \quad (26)$$

$$n \cdot (\sigma_i^* \nabla \nu + (\sigma_i^* + \sigma_e^*) \nabla u_e) = n \cdot (\sigma_T^* \nabla u_T), \quad \bar{x} \in \partial H; \quad (27)$$

$$n \cdot (\sigma_i^* \nabla \nu + \sigma_i^* \nabla u_e) = 0, \quad \bar{x} \in \partial H; \quad (28)$$

$$\bar{n} \cdot \sigma_T^* \nabla u_T = 0, \quad \bar{x} \in \partial T. \quad (29)$$

The equation (22) represents the system of ordinary differential equations (19)-(20) corresponding to the biophysical model of the cell. The equations (23)-(24) describe the excitation wave propagation in the heart tissue. The equation (25) describes the potential distribution in the human body. Boundary conditions on the surface of the heart are (26)-(28). Boundary conditions on the human body correspond to (29). The values related to $[\alpha]C_m$ are designated with an asterisk.

Results and Discussion

Figure 3 illustrates the logical structure of the program. The program consists of four modules: 1 is the module of numerical simulation based on the bidomain model of the heart; 2 is the module to configure the parameters of the bidomain model of the heart; 3 is the module to calculate the residual error of the "model" ECG and high resolution ECG signal; 4 is the module to continue the search for the minimum residual or to complete the program. The input data for the

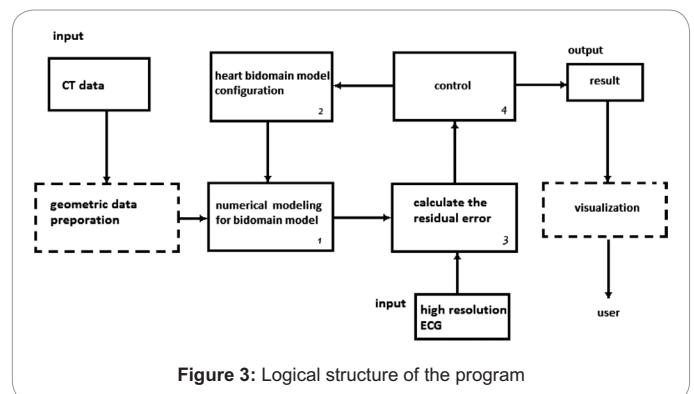


Figure 3: Logical structure of the program

program are the computed tomography data of the patient and the ECG signal recorded using the HSC to measure micropotentials of the heart.

The blocks designated by dotted lines are the external programs to perform service functions. The tomography image processing program and TetGen program are used to obtain the geometric data on the patient's heart and torso [6]. The tomography image processing program is used to prepare the data on both the internal and external surfaces of the heart muscle and the surface of the patient's torso. The TetGen program is the basic program to prepare the data to describe the finite element partitioning of the heart and torso.

The packages Cmgui [9] and Paraview [10] are used to visualize the results of the calculations.

The problem of finding the minimum error (residual error) between the model and measured ECG signal is generally solved. Module 1 is designed to generate the ECG signal on the basis of the results of numerical modeling of the heart activity in accordance with the mathematical model (19)-(26).

The class library developed in the framework of the project Chaste (Cancer, Heart and Soft Tissue Environment) is used in the model [11]. The project aims to create the software for modeling the biological objects and solve the problems arising in biology and physiology. While executing the project, the class libraries have been created by the body tissue modeling at the cellular level and at the level of tissues and organs. This software is based on the modern approaches of software engineering and the experience in developing the software for high performance computing in the field of computer modeling. The Chaste project is open and the members of the Computational Biology Group, Department of Computer Science, University of Oxford are mainly involved in the project [12].

The fundamental principles underlying the library are described in [13,14]. The main advantages of the library are unification of algorithms and their codes to solve the ordinary differential equations, partial differential equations and software implementation of the cell generation algorithms and formats of input-output data. It is important that the library is a free software with open source that allows its flexible use for computer modeling.

Most of the modules are written in the object-oriented programming language C++. This allows the creation of the applications with the efficient memory management and high performance and also provides a relatively simple modification and program code development.

The core of the class library is structured as follows:

- **global** contains the code for basic mathematical operations, time step organization, loading and saving the intermediate results, the classes for parallel work with vectors and the code to handle the errors;
- **io (input/output)** includes the modules for reading, writing and converting the data into a variety of other formats, including modules for working with HDF5 file formats [15], which enable hierarchical storage of the large amounts of digital data in a single file;
- **mesh** are the modules to generate the linear or quadratic tetrahedral cells, nodes, finite element, properties of the boundary surfaces, mesh generation; the package METIS/parMETIS is used for the spatial distribution of nodes of the finite element mesh; the libraries Triangle/TetGen, Meshalyzer, Cmgui and Paraview are used for the mesh data reading/writing and visualizing;

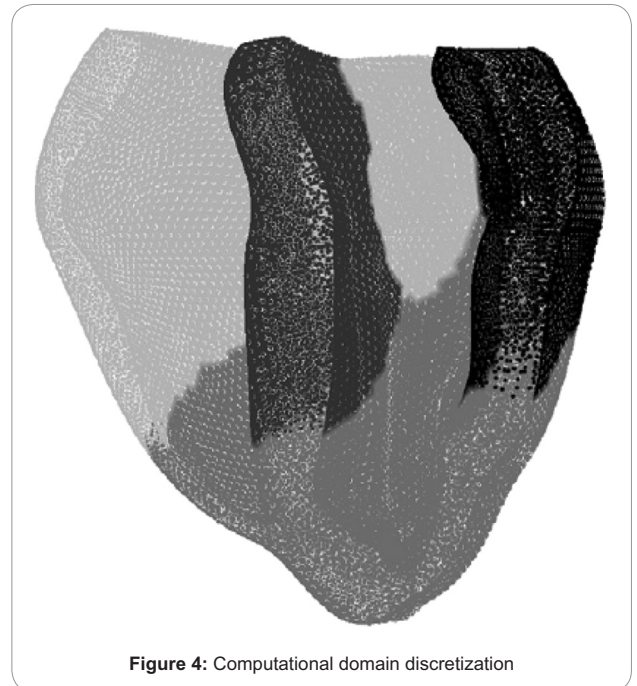


Figure 4: Computational domain discretization

- **linalg (linear algebra)** are the modules to convert matrices and vectors using the libraries Boost uBLAS [16] and PETSc [17];
- **ode** are the modules for numerical solution of the ordinary differential equations on the basis of the library Sundials CVODE [18,19];
- **pde** are the modules to solve the elliptic and parabolic equations of 2nd order using the method of finite elements.

To numerically solve the system (22)-(29), the computational domain (heart tissue) is divided into tetrahedral elements with vertices in N nodes. The level of detail of the heart tissue properties depends on the number of nodes. Figure 4 shows the ventricular cardiac tissue splitting that a priori allows solving the problem of localization of tissue of 2 mm in size. The required values can be written in the vector form $U^n = [V_1^n, \dots, V_N^n, u_{e1}^n, \dots, u_{eN}^n]^T$, where V_1^n and u_{e1}^n are transmembrane potential and extracellular potential, respectively, in the node number j and time step number n .

The finite element method brings the system of equations (22)-(29) at each time step to the system of linear equations:

$$AU^n = \bar{b}^n \quad (30)$$

Here, matrix A is time-independent, vector depends on the solution at the previous time step and ionic and external currents, and therefore varies in time. Thus, the calculation at each time step consists of the following stages:

1. Integration of the system of ordinary differential equations (ODE) (22) in each node, ODE solution.
2. Calculation of the vector of the right-hand sides
3. System solution (30).

At the first stage, the ionic currents are calculated on the basis of ODE solution (22). The system (22), or, in particular case, the Luo-Rudy model represents ten ordinary differential equations for the ionic currents and control variables. The studies in biophysics result in further

improvements of the cell models of different types, and thus the number of differential equations for transmembrane action potential is greater. Since the system is solved at each node of the mesh, it is important to use the optimal numerical method to reduce the calculation time. The Cauchy problem (19)-(21) is solved using the implicit Euler method. Write one differential equation of the system in the form of

$$\frac{dy_i}{dt} = f(y_1, y_2, \dots, t), \quad y_i(t_0) = y_{i0}, \quad i = 1, \dots, k \quad (31)$$

Here, $y_i(t)$ is the value of the desired function at time t (ionic current, control variable). Using time discretization, we obtain the dependence at $n+1$ st time step (Δt is time step):

$$y_i^{n+1} = y_i^n + \Delta t \cdot f(y_1^n, \dots, y_i^n, \dots, y_k^n, t_n) \quad (32)$$

The calculation method is determined by the form of the function $f(y_1, \dots, y_k, t)$. If the function is linear in the decision variable, y_i^{n+1} appears as calculation by the formula. If the function $f(y_1, \dots, y_k, t)$ is nonlinear, the root of nonlinear algebraic equation is found using the Newton-Raphson iterative method.

Formation of matrix A in (30) is based on the space and time discretization. Time discretization is performed using the partially implicit difference scheme. For example, for the equation

$$\frac{\partial u}{\partial t} = \nabla^2 u + f(u) \quad (33)$$

Time discretization is performed using the following scheme

$$\frac{u^{n+1} - u^n}{\Delta t} = \nabla^2 u^{n+1} + f(u^n) \quad (34)$$

Here, $n+1$ is the number of the next time step, Δt is the time step value. Space discretization is performed by the finite element method both for the elliptical (25) and parabolic equations (23)-(24) [20,21]. Partial differential equations (20)-(22) are written in the integral form in the variational formulation (in a "weak" form). Equation (23) takes the form:

$$\begin{aligned} & \frac{\chi C}{\Delta t} \int_H V^{n+1} \nu d\bar{x} + \int_H \sigma_i \nabla(V^{n+1} + u_e^{n+1}) \cdot \nabla \nu dx = \\ & = \frac{\chi C}{\Delta t} \int_H V^n \nu d\bar{x} - \int_H \chi I_{ion}(\bar{s}, V^n) \nu d\bar{x} + \int_{\partial H} I_i^{surf} \nu d\bar{x}, \quad \forall \nu \in V_0 \end{aligned} \quad (35)$$

Equation (24) takes the form:

$$\int_H (\sigma_i \nabla V^{n+1} + (\sigma_i + \sigma_e) \nabla u_e^{n+1}) \cdot \nabla \nu d\bar{x} = \int_{\partial H} (I_i^{surf} + I_e^{surf}) \nu d\bar{x}, \quad \forall \nu \in V_0 \quad (36)$$

Select N testing functions $\Psi_1, \Psi_2, \dots, \Psi_N$, represent the desired functions as $V = \sum_k \nu_k \Psi_k$ and $u_e = \sum_k \Phi_k \Psi_k$. Then, substitute ν for testing functions in the equations in variational formulation and obtain $2N$ equations. The first N equations have the form:

$$\frac{\chi C}{\Delta t} \overline{MV^{n+1}} + K[\sigma_i] \overline{V^{n+1}} + K[\sigma_i] \overline{\Phi^{n+1}} = \frac{\chi C}{\Delta t} \overline{MV^n} - \overline{MF^n} + \overline{c_{surf}} \quad (37)$$

Here, $\vec{V} = [V_1, V_2, \dots, V_N]$ and $\vec{\Phi} = [\Phi_1, \Phi_2, \dots, \Phi_N]$ are the values of the desired functions in the corresponding mesh nodes.

The elements of matrices M and K and vectors \vec{F} and $\overline{c_{surf}}$ are as follows:

$$\begin{aligned} M_{ij} &= \int_H \Psi_i \Psi_j d\bar{x}, & K[\sigma]_{ij} &= + \int_H \sigma_i \nabla \Psi_i \cdot \nabla \Psi_j d\bar{x} \\ F_j &= \int_H \Psi_j d\bar{x}, & c_j^{surf} &= \int_{\partial H} (I_i^{surf} + I_e^{surf}) \Psi_j d\bar{x} \end{aligned} \quad (38)$$

The next N equations have the form:

$$K[\sigma_i] \overline{V^{n+1}} + K[\sigma_i + \sigma_e] \overline{\Phi^{n+1}} = \vec{d}, \quad d_j = \int_{\partial H} (I_e^{surf} + I_i^{surf}) \Psi_j d\bar{x} \quad (39)$$

Finally, we get the system of linear equations in the form

$$\begin{pmatrix} \frac{\chi C}{\Delta t} M + K[\sigma_i] & K[\sigma_i] \\ K[\sigma_i] & K[\sigma_i + \sigma_e] \end{pmatrix} \begin{pmatrix} \overline{V^{n+1}} \\ \overline{\Phi^{n+1}} \end{pmatrix} = \begin{pmatrix} \frac{\chi C}{t} \overline{MV^n} - \overline{MF^n} + \overline{C_{surf}} \\ \vec{d} \end{pmatrix} \quad (40)$$

The algorithm of solving the system of linear equations (40) and peculiarities of implementing the finite element method of the heart activity modeling are presented in [21,22]. The program code for module 1 is entirely based on the class library to solve both the ordinary differential equations (ODESolver) and differential equations in partial derivatives (PDESolver) developed within the framework of the Chaste project.

The calculation of the residual error is performed in module 3 (Figure 3) using the following formulae. Let i denote the lead number. Then, $x_{gi}(t) = u_g(x_{1p}, y_{1p}, z_{1p}, t) - u_g(x_{2p}, y_{2p}, z_{2p}, t)$ is the measured potential difference on the patient's body between the points $(x_{1p}, y_{1p}, z_{1p}), (x_{2p}, y_{2p}, z_{2p}) \in \partial T$ at time t for the given lead.

Let $x_{mi}(t) = u_m(x_{1p}, y_{1p}, z_{1p}, t) - u_m(x_{2p}, y_{2p}, z_{2p}, t)$ denote the potential difference calculated with respect to the model for the same points of the body surface at time t . The value of $\delta_i^2 = \int_0^{t_i} (x_{gi}(\tau) - x_{mi}(\tau))^2 dt$ is to be used as the squared residual error for the lead number i . Then, $\delta^2 = \sum_i \delta_i^2$ is the squared total residual error.

Module 4 provides a step-by-step movement to the minimal residual error or decision to stop the program. Distribution of the heart tissue sections with different parameters of the cell models, different conductivity for the intracellular and extracellular spaces and orientation of the heart tissue fibers can be used as optimization parameters. The Gauss-Seidel method is used to find the optimum. A parameter of the model is changed at fixed values of all other parameters until the residual error is reduced. If the residual error decrease ceases, the given parameter is fixed and the other one starts changing.

The configuration files for module 1 are edited in module 2 according to the change of input parameters.

Conclusion

The optimal model of the electrical activity of the heart which enables investigation of the low-amplitude biopotentials causes has

been found. A generalized algorithm to study the heart model has been proposed for the hardware-software complex intended to detect the low-amplitude biopotentials of the heart, for example, VLPs arising due to the delayed ventricular depolarization. The class library created in the framework of the Chaste project was used to develop the computer model [11]. The main advantage of the library is the unification of algorithms and their codes for the ordinary and partial differential equations solution and software implementation of the mesh generation algorithms and the data input-output formats.

Acknowledgment

The research was financially supported by the Federal Targeted Programme “Research and Development in Priority Fields of S&T Complex of Russia in 2014-2020”, the Agreement No. 14.578.21.0032 dated 05.06.2014 “Development of the experimental sample of a hardware-software complex for noninvasive recording of heart micropotentials in a wide frequency band without filtering and averaging in real time to early detect the symptoms of a sudden cardiac death”; the unique identifier of the contract: RFMEF157814X0032.

References

1. Sundnes J, Terje G, Cai LX, Nielsen BF, *et al.* (2006) Computing the Electrical Activity in the Heart. Springer, p. 321. ISBN-13 978-3-540-33432-3.
2. Mandel WJ, ed. (1996) Cardiac Arrhythmias. Moscow: Medicine.
3. Bodin ON (2008) Systems of non-invasive control of the heart condition. Ph.D. dissertation. Penza.
4. Clayton RH, Bernus O, Cherry EM, Dierckx H, Fenton FH, *et al.* (2011) Models of cardiac tissue electrophysiology: progress, challenges and open questions. *Prog Biophys Mol Biol* 104: 22-48.
5. Avdeeva DK, Rybalka SA, Yuzhakov MM (2012) Development of the method to measure broadband signals of nanovolt and microvolt level for electrophysiological study. *Int J Appl Fund Res* 11: 37-38.
6. Technology Profile Date Views 01.01.2013. www.tetgen.org
7. CellML Date Views 01.01.2013. www.cellml.org/.
8. Luo CH, Rudy Y (1991) A model of the ventricular cardiac action potential: depolarisation, repolarisation, and their interaction. *Circ Res* 68: 1501-1526.
9. cmiss Date Views 01.01.2013. www.cmiss.org/cmgui
10. Cedilnik A, Geveci B, Moreland K, Ahrens J, Favre J (2006) Remote large data visualization in the paraview framework. *Eurogr Symp Parallel Graph Visualization*, pp. 163-170.
11. Cardiac Chaste: developing software for realistic heart simulations. Date Views 01.01.2013. www.cs.ox.ac.uk/chaste/cardiac_index.html
12. Computational Biology. Date Views 01.01.2013. www.cs.ox.ac.uk/research/compbio/
13. Mirams GR, Arthurs CJ, Bernabeu MO, Bordas R, Cooper J, *et al.* (2013) Chaste: an open source C++ library for computational physiology and biology. *PLoS Comput Biol* 9(3): e1002970. doi:10.1371/journal.pcbi.1002970.
14. Pitt-Francis J, Pathmanathan P, Bernabeu MO, Bordas R, Cooper J, *et al.* (2009) Chaste: a test-driven approach to software development for biological modelling. *Comput Phys Commun* 180(12): 2452-2471. doi:10.1016/j.cpc.2009.07.019.
15. Folk M, Cheng A, Yates K (1999) HDF5: a file format and I/O library for high performance computing applications. In: *Proc. Supercomputing*. Vol. 99. Key: citeulike:6765250.
16. Karlsson B (2005) Beyond the C++ Standard Library: An Introduction to Boost. Boston, MA: Addison-Wesley Professional.
17. Balay S, Gropp WD, L. C. McInnes, Smith BF (1997) Efficient management of parallelism in object oriented numerical software libraries. In: Arge E, Bruaset A, Langtangen H, eds. *Modern Software Tools in Scientific Computing*. Boston, MA: Birkhuser Press, pp. 163-202.
18. Sundials (SUite of Nonlinear and Differential/ALgebraic equation Solvers) Date Views 01.01.2013. [//computation.llnl.gov/casc/sundials/main.html](http://computation.llnl.gov/casc/sundials/main.html).
19. Hindmarsh C, Brown PN, Grant KE, Lee SL, Serban R, *et al.* (2005) SUNDIALS: Suite of nonlinear and differential/algebraic equation solvers. *ACM Trans Math Software* 31: 363-396. doi:10.1145/1089014.1089020.
20. Zienkiewicz OC, Taylor RL, Zhu JZ (2005) *The Finite Elements Method: Its Basis and Fundamentals* (6th ed.). Oxford: Elsevier Butterworth-Heinemann, p. 350. ISBN 978-0750663205.
21. Pathmanathan P (n.d.) Chaste: Finite Element Implementations. [//chaste.cs.ox.ac.uk/trac/wiki/ChasteGuides](http://chaste.cs.ox.ac.uk/trac/wiki/ChasteGuides)
22. Vazquez M, Arns R, Houzeaux G, Aubry R, Villar P, *et al.* (2011) A massively parallel computational electrophysiology model of the heart. *Int J Numer Meth Biomed Eng* 27: 1911-1929. doi:10.1002/cnm.1443.

Citation: Kazakov VY, Avdeeva DK, Grigoriev MG, Natalinova NM, Maksimov IV, *et al.* (2015) Electrodynamic Model of the Heart to Detect Necrotic Areas in a Human Heart. *Biol Med (Aligarh)* 7(5): BM-155-15, 7 pages.

Submit your next manuscript and get the following advantages

Special features:

- 30 days rapid review process
- Quality and quick editorial, review and publication processing
- Indexing at Scopus, EBSCO, ProQuest, Gale Cengage, and Google Scholar etc
- Authors, Reviewers and Editors rewarded with online Scientific Credits
- Better discount for your subsequent articles

Submit your manuscript at: submissions@biomedonline.com

